A Comparative Study on the Darrieus Turbine Blade Aerodynamics Applying Cascade Theory Including Boeing-Vertol and ECN Stall Models

A.C. Mandal[1]
J.D. Burton
Dept. of Engineering
University of Reading
Whiteknights P.O. Box 225
Reading RG6 2AY
U.K.

Abstract : A comparison of the theoretical investigation of the dynamic stalling effect on the aerodynamic performance of vertical-axis straight-bladed Darrieus wind turbines, is presented. To determine the performance characteristics, Boeing-Vertol and ECN stall models are added independently to the cascade method. Some improvements in the performance predictions of overall power coefficients and instantaneous blade forces are found for adding dynamic stall effect. From the comparison it is observed that Boeing-Vertol model shows better response.

Received : July 30,1994
Accepted : Nov. 15,1994

Keywords : *Darrieus Turbine, Dynamic Stall, Wind Energy.*

INTRODUCTION

In order to predict the performance characteristics of a Darrieus wind turbine properly, the effect of dynamic stalling need to be considered at the lower tip speed ratio. When the angle of attack remains constant or vary slowly with time, the turbine encounters the static stall. But when the angle of attack changes rapidly with time, the turbine experiences the dynamic stall. There are substantial differences between the characteristics of the static and dynamic stalls. The dynamic stall is a complex and unsteady flow phenomena. Aerodynamic forces due to the dynamic stall may be much higher than those due to the static stall. As result, for the performance prediction of Darrieus turbines, especially for the local forces, there appear substantial differences between the experimental data and the calculated values unless the dynamic stalling effect is added.

A number of performance prediction models of Darrieus wind turbines have been applied till today in many places. Among them, the three main models are :

Present Address
[1]*Dept. of Mechanical Engineering, BUET, Dhaka-1000, Bangladesh.*

momentum model, vortex model and cascade model. Each of the models has got some deficiencies.

Strickland (Strickland, 1975) introduced the momentum model which can only be applied reasonably for the prediction of the overall performance characteristics of a low solidity Darrieus wind turbine. This model offers limitation with regard to its convergence problem at high tip speed ratio and high solidity. Strickland, Webster and Nguyen (Strickland et al, 1979) introduced the vortex model which cannot always be used properly for the prediction of performance characteristics. This model often creates convergence problem and in addition it takes very large computation time. Hirsch and Mandal (Hirsch and Mandal, 1987) introduced the cascade model which can be used reasonably for the performance prediction of Darrieus turbines at all practical tip speed ratios and solidities. However, some shortcomings in regard to its prediction of the instantaneous blade forces and wake velocities are found. To improve this situation the effect of dynamic stalling is added to the cascade model.

With a view to incorporate the effect of dynamic stall, two different stall models such as, Boeing-Vertol stall model (Gormont, 1973) and the ECN stall model (Bulteel, 1987-88) are added independently to the cascade theory. To simplify the analysis and eliminate the deficiency associated with the Boeing-Vertol stall model, some modifications are made : one for lift characteristics in the prestall condition and another for the drag characteristics. In the ECN stall model the expression of the drag coefficient is modified in the similar manner as that for the Boeing-Vertol stall model.

The effects of zero-lift-drag coefficient (Hirsch and Mandal, 1984) and the finite blade aspect ratio (Clancy, 1978) are also encountered in the analysis. Two dimensional aerodynamic lift-drag characteristics for the static condition are taken from the references (Jacob and Sherman, 1937), (Sheldahl and Blackwell, 1976) and (Willmer, 1979). Comparisons of the experimental data and the calculated values are made and it is observed that for adding dynamic stall effect with the cascade model there have been some improvements in the performance predictions.

BOEING-VERTOL STALL MODEL

In the model of Boeing-Vertol (Gormont, 1973), the blade angle is modified. The modified angle of attack α_d (dynamic angle of incidence) is determined from the following relation,

$$\alpha_d = \alpha - \gamma k_1 \left(\sqrt{\left|\frac{C\alpha}{2W}\right|} \right) S_\alpha \qquad (1)$$

where α is the effective blade angle of attack, γ and k_1 are the empirical constants, α denotes the instantaneous rate of change of α, S_α is the sign of α and W is the relative flow velocity. This modified angle of attack is used to calculate the lift coefficient due to the dynamic stalling effect C_{ld} in the following manner,

$$C_{ld} = \left(\frac{\alpha}{\alpha_d}\right) C_1(\alpha_d) \qquad (2)$$

where $C_1(\alpha_d)$ is the lift value chosen corresponding to the modified angle of attack α_d and the value is taken from the two-dimensional lift characteristics with static stall condition. For low Mach Numbers and the aerofoil thickness to chord ratios greater than 0.1, the value of γ is,

$$\gamma = 1.4 - 6\,(0.06 - t_c) \qquad (3)$$

where t_c is the maximum aerofoil thickness ratio. The k_1 value changes with the sign of the effective angle of attack and this is obtained from the relation.

$$k_1 = 0.75 + 0.25 \times S_\alpha \qquad (4)$$

This formulation is applied (Gormont, [5]) when the angle of attack α is greater than the static stall angle or when the angle of attack is decreasing after having been above the stall angle. The Boeing-Vertol stall model is turned off when the angle of attack is below the stall angle and increasing. For the present analysis in the prestall condition, the dynamic stalling effect is also encountered from α = 5 degree upto the stall angle in the similar manner as that of ECN (Bultal, 1987-88). The dynamic lift C_{ld} is calculated by using the Boeing-Vertol model and according to ECN, the lift coefficient in the prestal condition is obtained from the relation,

$$C_{lp} = P_f\, C_{ld}(\alpha_d) + (1 - P_f)\, C_1(\alpha) \qquad (5)$$

where, the factor P_f is determined from the following linear equation,

$$P_f = (\alpha\text{-}5)/(\alpha_s - 5) \tag{6}$$

where α_s is the stalling angle. This equation reveals that at $\alpha = 5$ degree, P_f is zero and at $\alpha = \alpha_s$, P_f is unity, which mean that at $\alpha = 5$ degree, the contribution of C_{ld} is zero while at $\alpha = \alpha_s$, it is full.

In the analysis to consider the effect of drag characteristics due to the dynamic stall, an empirical relation (Maniruzzaman and Mandal, 1993) is used which is written in the form,

$$C_{dd} = \frac{C_{ld}}{C_l(\alpha)} C_d(\alpha) K \tag{7}$$

where K is a factor. K is chosen as 1.0 in this expression. The equation (7) signifies that, the dynamic drag characteristic is proportional to the dynamic lift characteristic. Due to lack of experimental drag values, the calculated dynamic drag characteristics cannot be verified at the moment. However, the nature of this equation more or less follows that presented by Mc Crosky (Mc Crosky et al, 1982) and opposes the nature which is given by Mehta (Mehta, 1977). Mc Crosky considered the viscous flow while Mehta considered the ideal flow in their analyses.

ECN STALL MODEL

The ECN stall model is introduced by Bulteel (Bulteel, 1987-88). In this model, the dynamic stall delay angle (in degrees) is expressed as follows,

$$\Delta\alpha_d = 74.5 \sqrt{\left|\frac{C\alpha}{2W}\right|} + 4.47 \tag{8}$$

The expression of dynamic angle of incidence is given as,

$$\alpha_d = [\,|\alpha| - G\Delta\alpha_d]\, S_\alpha \tag{9}$$

where G is a constant which can be defined as,

$G = 1$ for $\alpha \geq 0$ and $G = 0.5$ for $\alpha < 0$

An intermediate lift coefficient is defined as,

$$C_{li}\ (\alpha_d) = \frac{\alpha}{\alpha_d}\ C_1\ (\alpha_d) \qquad (10)$$

The dynamic lift coefficient is defined by linear combination

$$C_{ld} = P_f\, C_{1i}\,(\alpha_d) + (1 - P_f)\, C_1\,(\alpha) \qquad (11)$$

$P_f = P_f\,(\alpha, \alpha_s)$ is defined so that the hysteresis appears near the stationary stall.

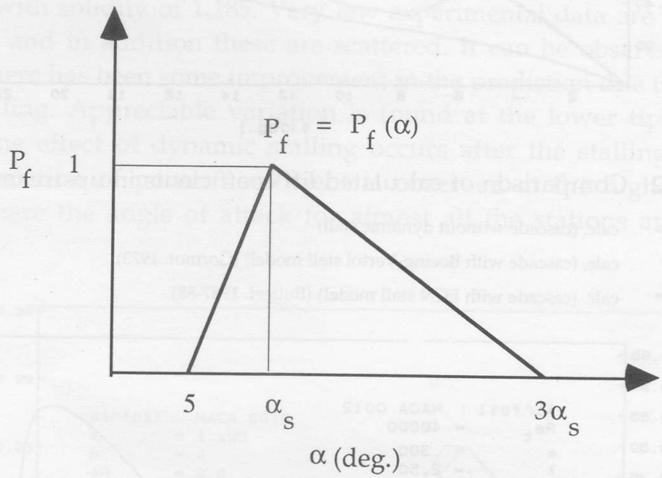

Figure 1 : The variation of P_f vs. α.

In this model modification is done in the expression of the drag coefficient. The drag coefficient is obtained from the equation (7) in the similar manner as that obtained for the Boeing-Vertol stall model.

RESULT AND DISCUSSION

Figures 2 and 3 show respectively the comparisons of the static and dynamic lift and drag characteristics. It is observed from these Figures that there has been significant difference between the static and dynamic lift and drag-characteristics. It occurs due to completely different flow phenomena in the case

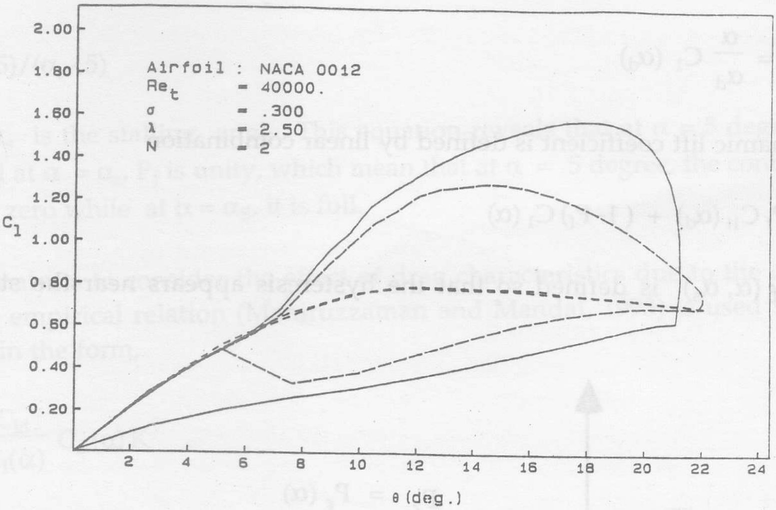

Fig. 2 Comparison of calculated lift coefficients in upstream side.

calc. (cascade without dynamic stall)

calc. (cascade with Boeing-Vertol stall model) (Gormot. 1973)

calc. (cascade with ECN stall model) (Bulteel. 1987-88)

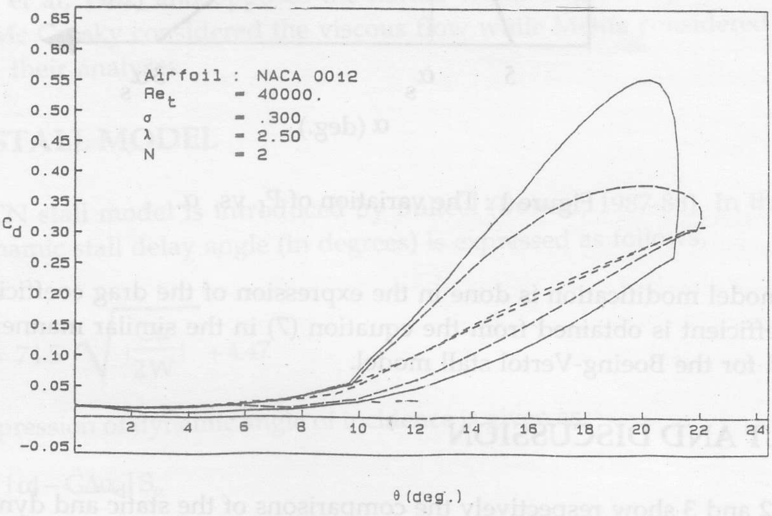

Fig. 3 Comparison of calculated drag coefficients in upstream side.

calc. (cascade without dynamic stall)

calc. (cascade with Boeing-Vertol stall model) (Gormot. 1973)

calc. (cascade with ECN stall model) (Bulteel. 1987-88) of dynamic stalling condition (Mehta, 1977). One can observe from Figures 2 and 3 that the influence of dynamic stalling by the Boeing-Vertol model is higher than that by the ECN model. In both the models during rising the angle of attack, the lift and drag characteristics increase while they drop with lowering angle of attack which is vivid from Figures 2 and 3.

In Figure 4, the comparison of the calculated values of overall power coefficient and the experimental data from the Reading University (Mays and Musgrove, 1979), is shown. The running speed of the turbine varies from 3 to 7 m/s. So, in the present calculation mean wind speed Reynolds Number of 138000 is considered for this turbine with solidity of 1.185. Very few experimental data are available for their turbine and in addition these are scattered. It can be observed from this Figure that there has been some improvement in the prediction due to addition of dynamic stalling. Appreciable variation is found at the lower tip speed ratio side. Since the effect of dynamic stalling occurs after the stalling angle very negligible variation of power coefficient is observed at the higher tip speed ratio side where the angle of attack for almost all the stations are below the stalling angle.

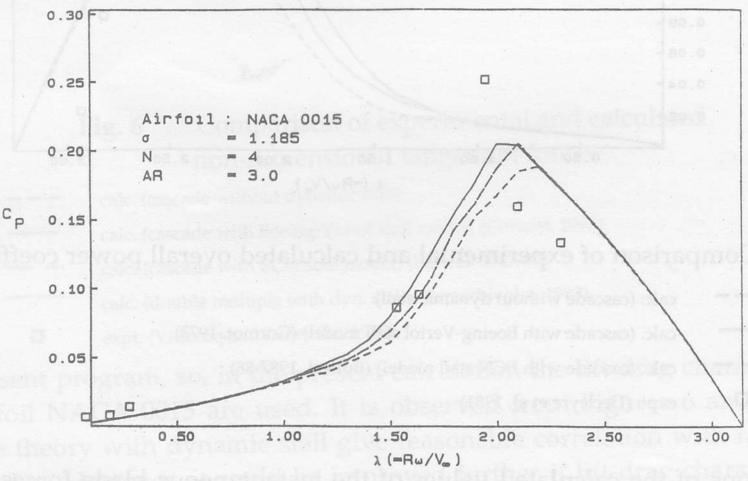

Fig. 4 Comparison of experimental and calculated overall power coefficients.

— — — calc. (cascade without dynamic stall)

——— calc. (cascade with Boeing-Vertol stall model) (Gormot. 1973)

—— — calc. (cascade with ECN stall model) (Bulteel. 1987-88)

□ expt. (Mays and Musgrove, 1979)

Figure 5 show the comparison of the calculated overall power coefficients and the experimental data of the VUB wind tunnel test model (Decleyre et al, 1981). The model test was conducted at the constant wind speed of 7.28 m/s. From this Figure it is seen that there has been some increase of power coefficient value at the lower tip speed ratio side due to the effect of dynamic stalling. At the higher tip speed ratio very negligible change is observed. The phenomenon can be described in the similar way as for the Figure 4. It is further observed that, the effect of dynamic stalling by Boeing-Vertol model is greater than that by the ECN model. For adding dynamic stalling improvement in the power coefficient is observed from this figure.

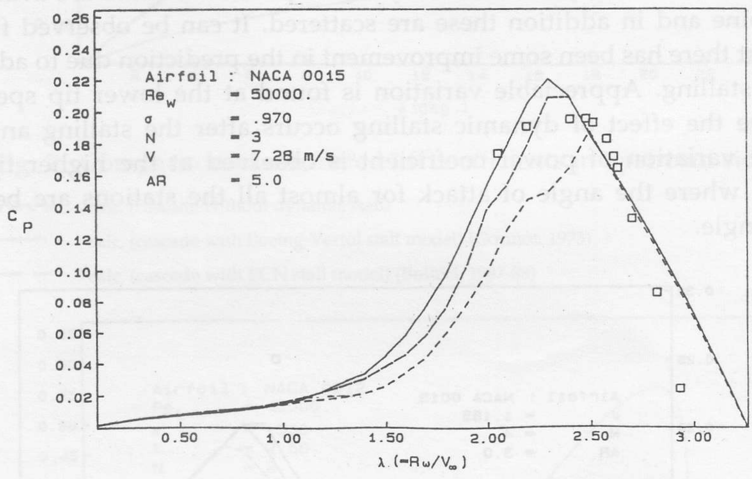

Fig. 5 Comparison of experimental and calculated overall power coefficients.

- - - calc. (cascade without dynamic stall)

—— calc. (cascade with Boeing-Vertol stall model) (Gormot. 1973)

— — calc. (cascade with ECN stall model) (Bulteel. 1987-88)

□ expt. (Decleyre et al, 1981)

Comparisons of the calculated values of the instantaneous blade forces and the experimental data from the university of Sherbrooke (Vittecoq and Laneville, 1982) are shown in Figures 6 and 7. The available calculated values of the instantaneous blade forces by the double multiple streamtube method with dynamic stall effect (Paraschivoiu, 1983) are also plotted for the comparison. Since, the lift drag characteristic of the airfoil NACA 0018 are not available in

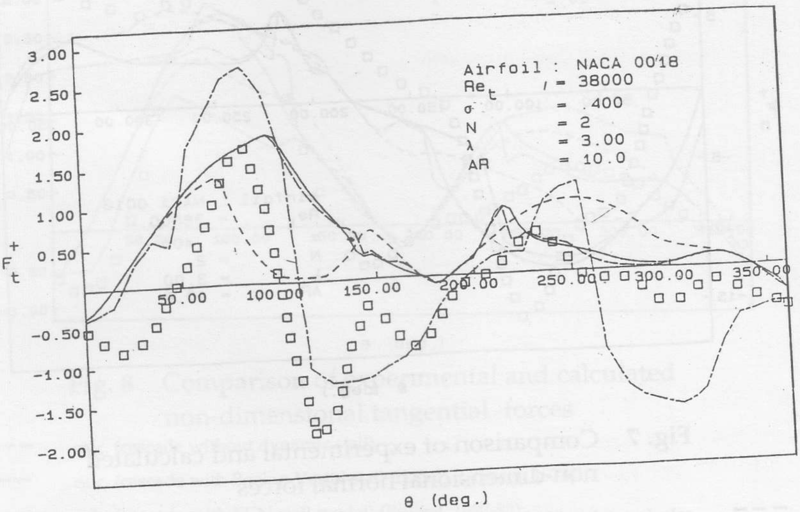

Fig. 6 Comparison of experimental and calculated non-dimensional tangential forces

- calc. (cascade without dynamic stall)
- calc. (cascade with Boeing-Vertol stall model) (Gormot. 1973)
- calc. (cascade with ECN stall model) (Bulteel. 1987-88)
- calc. (double multiple with dyn. stall) (Paraschivoiu., 1983)
- expt. (Vittecoq and Laneville, 1982)

the present program, so, in the present calculation the lift drag characteristics of the airfoil NACA 0015 are used. It is observed from Figures 6 and 7 that the cascade theory with dynamic stall give reasonable correlation with regard to its peak value. However, it could be improved further if lift-drag characteristics of airfoil NACA 0018 would be used. Based on overall considerations, it may be concluded that the range of uncertainty shall be of the order of 5% for using the lift-drag characteristics of the airfoil NACA 0015 in place of those of the airfoil NACA 0018.

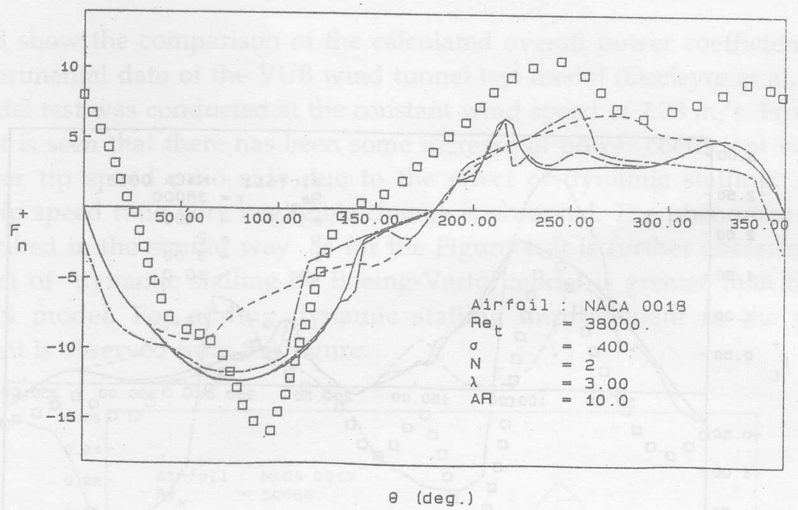

Fig. 7 Comparison of experimental and calculated non-dimensional normal forces

- - - calc. (cascade without dynamic stall)

——— calc. (cascade with Boeing-Vertol stall model) (Gormot. 1973)

— — calc. (cascade with ECN stall model) (Bulteel. 1987-88)

—·— calc. (double multiple with dyn. stall) (Paraschivoiu., 1983)

□ expt. (Vittecoq and Laneville, 1982)

Figures 8 to 11 show the comparisons of the calculated instantaneous blade forces and the experimental data from the Sandia Laboratories (Strickland et al, 1981). They present the water two tank data for a straight bladed Darrieus turbine with the blade airfoil NACA 0012. The available calculated values by the dynamic vortex model (Strickland et al, 1981) and those by the quasi-steady vortex model (Strickland et al, 1979) are also considered for comparison.

It is observed from Figures 8 to 11 that for adding the effect of dynamic stalling to the cascade model, there has been appreciable improvement in the prediction of the instantaneous blade forces. If can be observed that the correlation with the calculated values by the dynamic vortex model is not always consistent, in some places it is reasonable and in some places over prediction is seen. On the other hand, the calculated values by the quasi-steady vortex model always give under prediction. Due to the addition of the dynamic stall, the net values of the lift coefficients increase in the upstream side and decrease in the downstream side, as a result the tangential and normal forces increase in the upstream side and decrease in the downstream side in general.

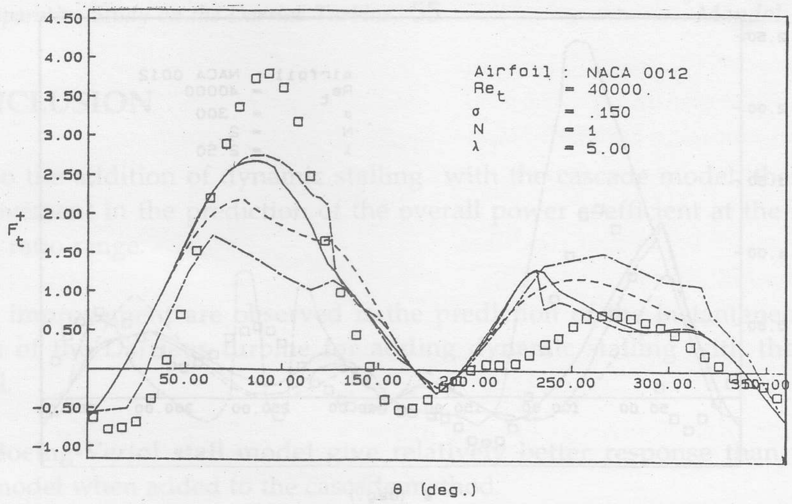

Fig. 8 Comparison of experimental and calculated non-dimensional tangential forces

- - - calc. (cascade without dynamic stall)
—— calc. (cascade with Boeing-Vertol stall model) (Gormot. 1973)
— — calc. (cascade with ECN stall model) (Bulteel. 1987-88)
—·— calc. (quasi-steady vortex) (Strickland et al. 1979)
□ expt. (Strickland et al. 1981)

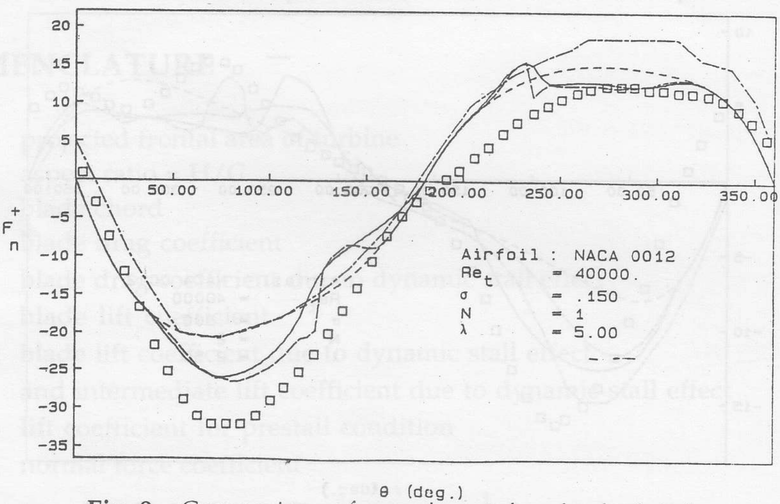

Fig. 9 Comparison of experimental and calculated non-dimensional normal forces

- - - calc. (cascade without dynamic stall)
—— calc. (cascade with Boeing-Vertol stall model) (Gormot. 1973)
— — calc. (cascade with ECN stall model) (Bulteel. 1987-88)
—·— calc. (quasi-steady vortex) (Strickland et al. 1979)
□ expt. (Strickland et al. 1981)

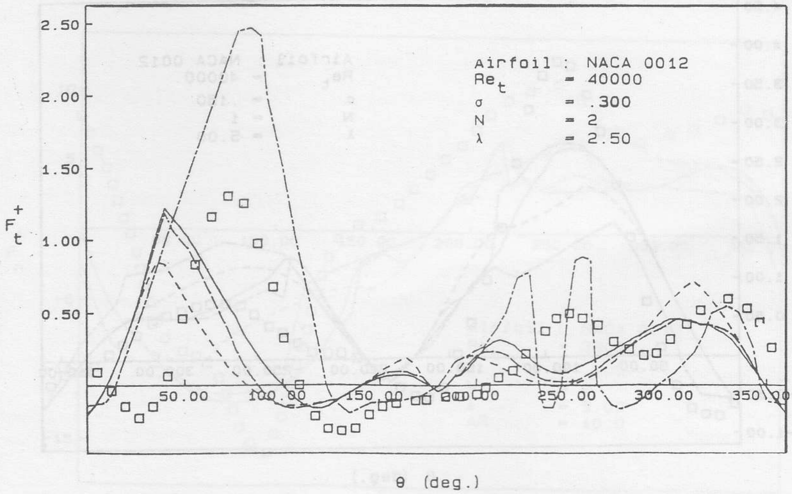

Fig. 10 Comparison of experimental and calculated non-dimensional tangential forces

- - - calc. (cascade without dynamic stall)
——— calc. (cascade with Boeing-Vertol stall model) (Gormot. 1973)
— — calc. (cascade with ECN stall model) (Bulteel. 1987-88)
—·— calc. (dynamic vortex model) (Strickland et al. 1981)
□ expt. (Strickland et al. 1981)

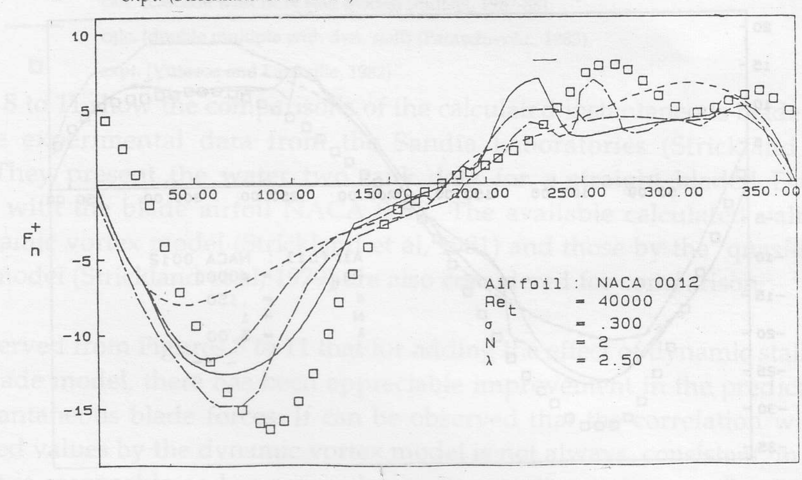

Fig. 11 Comparison of experimental and calculated non-dimensional normal forces

- - - calc. (cascade without dynamic stall)
——— calc. (cascade with Boeing-Vertol stall model) (Gormot. 1973)
— — calc. (cascade with ECN stall model) (Bulteel. 1987-88)
—·— calc. (dynamic vortex model) (Strickland et al. 1981)
□ expt. (Strickland et al. 1981)

CONCLUSION

Due to the addition of dynamic stalling with the cascade model, there occurs improvement in the prediction of the overall power coefficient at the lower tip speed ratio range.

Some improvement are observed is the prediction of the instantaneous blade forces of the Darrieus turbine for adding dynamic stalling with the cascade model.

The Boeing-Vertol stall model give relatively better response than the ECN stall model when added to the cascade method.

At the present moment sufficient experimental data are not available to check the expressions of lift-drag characteristics including dynamic stalling effect. These are necessary to make further comparisons.

For further improvement in the correlation, other important effects such as, flow curvature, added mass etc. may be added to the cascade method in addition.

NOMENCLATURE

A	projected frontal area of turbine
AR	aspect ratio = H/C
C	blade chord
C_d	blade drag coefficient
C_{dd}	blade drag coefficient due to dynamic stall effect
C_l	blade lift coefficient
C_{ld}	blade lift coefficient due to dynamic stall effect
C_{li}	and intermediate lift coefficient due to dynamic stall effect
C_{lp}	lift coefficient for prestall condition
C_n	normal force coefficient
C_p	turbine overall power coefficient = $P_o/\frac{1}{2}\rho A V_\infty{}^3$
C_t	tangential force coefficient
$F_n{}^+$	non-dimensional normal force = $C_n\,(W/V_\infty)^2$
$F_t{}^+$	non-dimensional tangential force = $C_t\,(W/V_\infty)^2$
G	a constant

H	height of turbine
k_1	an empirical constant
K	factor to include dynamic stall
N	number of blades
P_f	a factor in prestall condition
P_o	overall power
R	turbine radius
Re_t	turbine speed Reynolds Number = $R\omega C/\nu$
Re_W	wind speed Reynolds Number = $V_\infty C/\nu$
S_α	sign of rate of change of angle of attack
t_c	maximum blade thickness as a fraction of chord
V_∞	wind velocity
W	relative flow velocity
α	effective blade angle
α	instantaneous rate of change of α
α_d	dynamic angle of incidence
α_s	stalling angle
γ	an empirical constant
$\Delta\alpha_d$	dynamic stall delay angle
θ	azimuth angle
λ	tip speed ratio = $R\omega/V_\infty$
ν	kinematic viscosity
ρ	fluid density
σ	solidity = NC/R
ω	angular velocity of turbine in rad/sec

REFERENCES

1. Bulteel, D., *Centrifugalbeveiliging van een vertikale as windturbine*, VUB Fakulteit Toegepaste Wetenschappen, Brussel, 1987-88.

2. Clancy, L.J., *Aerodynamics*, A Pitman International Text, 2nd Edition, 1978.

3. Decleyre, W., Aerschot, D.V. and Hirsch, Ir. Ch., *The effects of Reynolds Number on the performance characteristics of Darrieus windmills with*

troposkien and straight-blades,, Proceedings of the International Colloquium on wind energy, Brighton, 243-248, 1981.

4. Ericsson, L.E. and Reding, J.P., *Engineering analysis of dynamic stall*, Proceedings of the ASME winter annual meeting, San Francisco, Calif., 117-123, 1978.

5. Gormont, R.E., *A mathematical model of unsteady aerodynamics and radial flow for application to helicopter rotors*, U.S. Army air mobility R&D laboratory, Vertol Division, Philadelphia, pa., Report on Boeing-Vertol contract DAA JOV-71-C-0045, 1973.

6. Hirsch, Ir.Ch. and Mandal, A.C., *Flow curvature effect on vertical axis Darrieus wind turbine having high chord-radius ratio*, Proceedings of the 1st European wind energy conference, Hamburg, 405-410, 1984 .

7. Hirsch, Ir.Ch. and Mandal, A.C., *A cascade theory for the aerodynamic performance of Darrieus turbines*, Wind Engineering, Vol. 11(3), 164-175, 1987.

8. Jacob, E.N. and Sherman, A., *Airfoil characteristics as affected by variations of the Reynolds Number*, NACA-TR-586, 1937.

9. Maniruzzaman, Md. and Mandal, A.C., *An investigation of the effect of dynamic stall on Darrieus turbines applying the cascade model*, RERIC international energy journal, AIT, Vol. 15(2), 111-123, 1993.

10. Mays, I.D. and Musgrove, P.J., *Performance of the variable geometry vertical axis wind turbine at high and low solidities*, Proceedings of the 1st wind energy association workshop, 48-56, 1979.

11. McCroskey, W.J. and Pucci, S.L., *Viscous inviscid interaction on oscillating airfoils in subsonic flow*, AIAA Journal, Vol. 20, 167-174, 1982.

12. Mehta, U.B., *Dynamic stall on an oscillating airfoil*, Proceedings of AGARD fluid dynamics panel symposium on unsteady aerodynamics, AGARD CPP-227, 1977.

13. Paraschivoiu , I., *Predicted and experimental aerodynamic forces on the Darrieus rotor*, Journal of energy, Vol. 7(6), 610-615, 1983.

14. Sheldahl, R.E. and Blackwell, B.F., *Aerodynamic characteristics of four symmetrical airfoil sections through 180 degrees angle of attack at low Reynolds Number*, Proceedings of the Vertical-axis wind turbine

technology workshop, Sandia laboratories, SAND76-5586, II-73-106, 1976.

15. Strickland, J.H., *The Darrieus turbine : a performance prediction model using multiple streamtubes*, Sandia laboratories report, SAND 75-0431, 1975.

16. Strickland, J.H., Smith, T. and Sun, K., *A vortex model of the Darrieus turbine : An analytical and experimental study*, Sandia laboratories report, SAND 81-7017, 1981.

17. Strickland, J.H., Webster, B.T. and Nguyen, T., *A vortex model of the Darrieus turbine : an analytical and experimental study*, Journal of fluids Engineering, Vol. 101 (4), 500-505, 1979.

18. Vittecoq, P. and Laneville, A., *Etude en soufflerie d'un rotor du type Darrieus*, Mechanical Engineering Department, University of Sherbrooke, Canada, Report MEC-82-2, 1982.

19. Willmer, A.C., *Low Reynolds Number tests on the NACA 0015 section*, Proceedings of the 1st British wind energy association workshop, 109-116, 1979.